Evidence for Pleistocene Low-Angle Normal Faulting in the Annapurna-Dhaulagiri Region, Nepal

Author(s): Jeni A. McDermott, Kip V. Hodges, Kelin X Whipple, Matthijs C. van Soest, and Jose M. HurtadoJr.

Source: *The Journal of Geology*, Vol. 123, No. 2 (March 2015), pp. 133-151
Published by: The University of Chicago Press
Stable URL: http://www.jstor.org/stable/10.1086/681219
Accessed: 29/10/2015 18:33

Evidence for Pleistocene Low-Angle Normal Faulting in the Annapurna-Dhaulagiri Region, Nepal

Jeni A. McDermott,[1,*] *Kip V. Hodges,*[1] *Kelin X Whipple,*[1] *Matthijs C. van Soest,*[1] *and Jose M. Hurtado Jr.*[2]

1. School of Earth and Space Exploration, Arizona State University, Tempe, Arizona 85287, USA;
2. Department of Geological Sciences, University of Texas at El Paso, El Paso, Texas 79968, USA

ABSTRACT

North-south-directed extension on the South Tibetan Fault System (STFS) played an important role in Himalayan tectonics of the Miocene Period, and it is generally assumed that orogen-perpendicular extension ceased in this orogenic system before the Pliocene. However, previous work in the Annapurna and Dhaulagiri Himalaya of central Nepal revealed evidence for local Pleistocene reactivation of the basal STFS structure in this area (the Annapurna Detachment). New structural mapping and (U-Th)/He apatite and zircon thermochronology in this region further document the significance of Pleistocene N-S extension in this sector of the Himalaya. Patterns of (U-Th)/He accessory-mineral ages are not disrupted across the reactivated segment of the STFS basal detachment, indicating that Pleistocene offset was limited. In contrast, the trace of a N-dipping, low-angle detachment in the hanging wall of the reactivated Annapurna Detachment—formerly linked to the STFS, but here named the Dhaulagiri Detachment—coincides with an abrupt break in the cooling-age pattern in two different drainages ~20 km apart, juxtaposing Miocene hanging-wall dates against Pleistocene footwall dates. Our observations, combined with previous fission-track data from the region, provide direct evidence for significant N-S extension in the central Himalaya as recently as the Pleistocene.

Online enhancements: appendix, tables.

Introduction

The Himalayan-Tibetan orogenic system provides an unusual opportunity to examine the role of extensional faulting in the evolution of collisional orogens. The South Tibetan Fault System (STFS; fig. 1*A*), a family of predominantly top-to-the-north normal faults, can be traced for more than 2000 km along strike near the crest of the range (e.g., Burchfiel et al. 1992). The STFS, along with contemporaneous thrusting on the structurally lower Main Central Thrust System, is thought to be responsible for the exhumation of the core of the Himalaya in the Early to Middle Miocene (Hodges et al. 1992, 1996; Nazarchuk 1993; Coleman 1996; Coleman and Hodges 1998; Searle et al. 1999). While it is widely perceived that slip on the STFS ceased by the Middle Miocene (e.g., Searle and Godin 2003), N-S-directed extensional faulting across the Himalayan crest is not limited to Miocene strands of the STFS. Quaternary displacement on E-W- to NW-SE-striking, shallowly to moderately N-dipping faults with variable components of northward displacement has been documented near the range crest in several regions spanning a distance of more than 600 km across the central Himalaya. Some of these faults have been interpreted previously as part of the STFS (Wu et al. 1998; Hurtado et al. 2001), while others transect the Miocene structural grain of the Himalaya and have been regarded as distinctive (Nakata 1989; McDermott et al. 2013; Murphy et al. 2014). The tectonic significance of this young extensional faulting has not been established with confidence because of uncertainties in the regional extent of individual fault strands, a general lack of direct constraints on the timing of faulting, and the absence of estimates

Manuscript received July 15, 2014; accepted February 19, 2015; electronically published March 25, 2015.

* Author for correspondence. Present address: Department of Geology, University of St. Thomas, St. Paul, Minnesota 55105, USA; e-mail: jamcdermott@stthomas.edu.

[The Journal of Geology, 2015, volume 123, p. 133–151] 0022-1376/2015/12302-0003$15.00. DOI:10.1086/681219

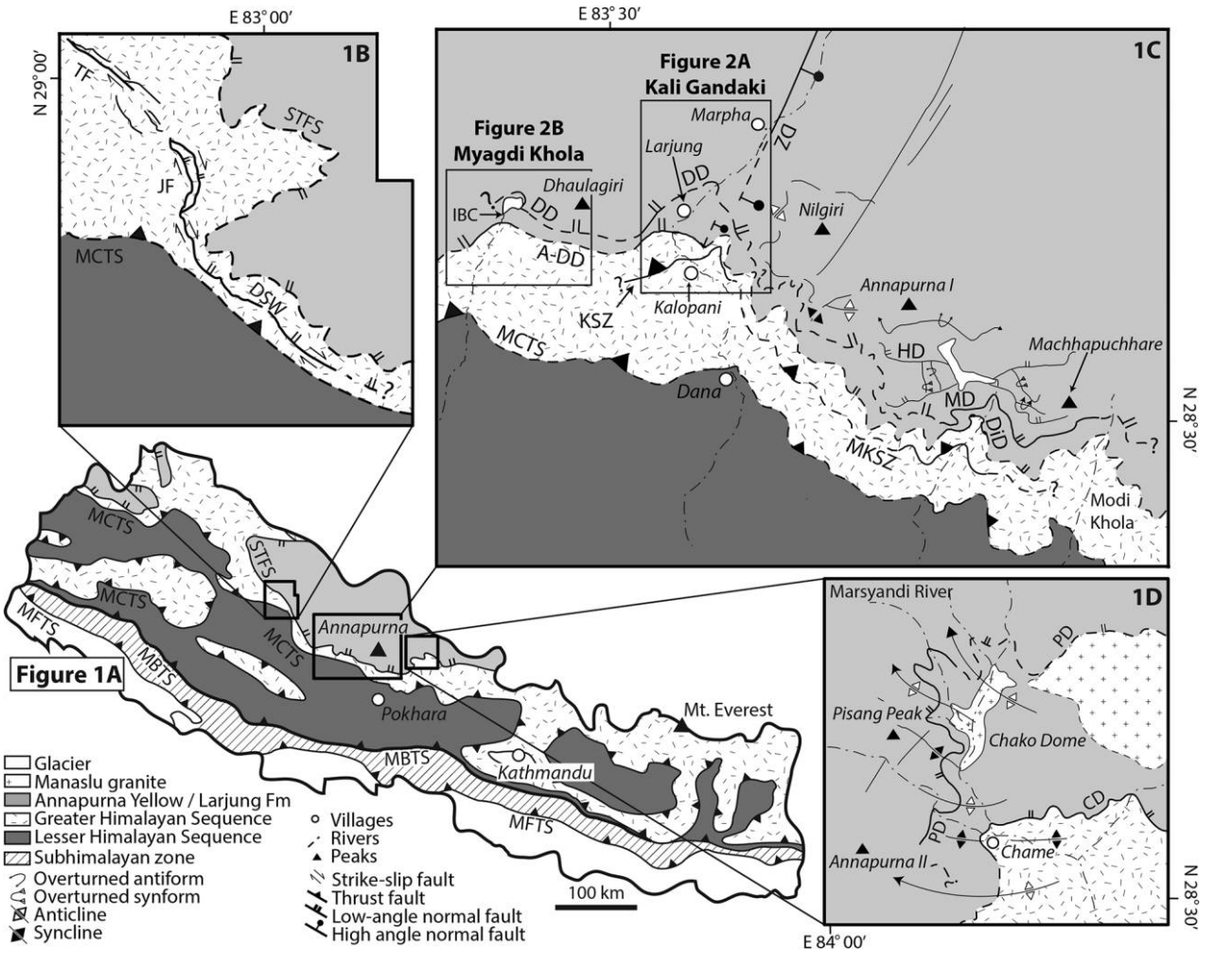

Figure 1. Geologic and structural maps of selected locations across central Nepal discussed in the text, modified from Colchen et al. (1986), Vannay and Hodges (1996), Hurtado et al. (2001), Godin (2003), and Silver (2012). *A*, Generalized geologic map of Nepal, showing spatial relationship of discussed locations; *B*, large-scale map of the western Dhaulagiri Himalaya, encompassing the Dhaulagiri Transtensional Zone (Silver 2012), including the Dhaulagiri Southwest Fault (Nakata 1989); *C*, detailed map of the eastern Dhaulagiri Himalaya and the Annapurna Himalaya, showing the extent of the study areas, the Kali Gandaki Valley (right-hand inset, fig. 2*A*) and Myagdi Khola Valley (left-hand inset, fig. 2*B*). The Modi Khola Valley is also shown to the immediate west of Machhapuchhare; *D*, Marsyandi Valley of the eastern Annapurna Himalaya. Abbreviations: A-DD = Annapurna-Dhumpu Detachment; CD = Chame Detachment; DD = Dhaulagiri Detachment; DiD = Deorali Detachment; DSW = Dhaulagiri Southwest Fault; DZ = Dangardzong Fault; HD = Hiunchuli Detachment; IBC = Italian base camp; JF = Jangla Fault; KSZ = Kalopani Shear Zone; MBTS = Main Boundary Thrust System; MCTS = Main Central Thrust System; MD = Machhapuchhare Detachment; MFTS = Main Frontal Thrust System; MKSZ = Modi Khola Shear Zone; PD = Phu Detachment; STFS = South Tibetan Fault System; TF = Tibrikot Fault.

of slip magnitude on many strands. If regional, N-S-directed extension is not limited to the Early to Middle Miocene but rather has played an important role in the subsequent evolution of the Himalaya, then current models of Late Miocene–Quaternary Himalayan tectonics are incomplete. Here we present thermochronologic evidence for significant displacement more recently than 1.5 Ma on a well-exposed N-dipping extensional structure in the Annapurna and Dhaulagiri Himalaya of Nepal.

Geologic Context

The terms "Dhaulagiri Himalaya" and "Annapurna Himalaya" refer to two clusters of mountains in central Nepal surrounding the seventh- and tenth-

highest peaks in the world: Dhaulagiri I at 8167 m and Annapurna I at 8091 m. The two are separated by one of our planet's deepest valleys, carved by the Kali Gandaki River (fig. 1*C*). From headwaters on the physiographic Tibetan Plateau, the low-gradient upper reaches of the Kali Gandaki flow along the floor of the N-S-trending Thakkhola Graben, one of numerous extensional features in the southern plateau formed in Miocene time and active into the Quaternary (Armijo et al. 1986; Coleman and Hodges 1995; Hurtado et al. 2001; Garzione et al. 2003). A prominent knickpoint in the river channel occurs near the southern termination of the graben in an area of massive landsliding. South of this knickpoint, the stream gradient increases dramatically as the Kali Gandaki carves a deep and narrow gorge through the physiographic Greater Himalaya between the Annapurna and Dhaulagiri Massifs. One key field site for our study was the area of this transition in the Kali Gandaki Valley, because it corresponds closely with the trace of the basal STFS structure (fig. 2*A*). Building on earlier work by Hurtado et al. (2001) that yielded evidence for Quaternary slip along a reactivated segment of this struc-

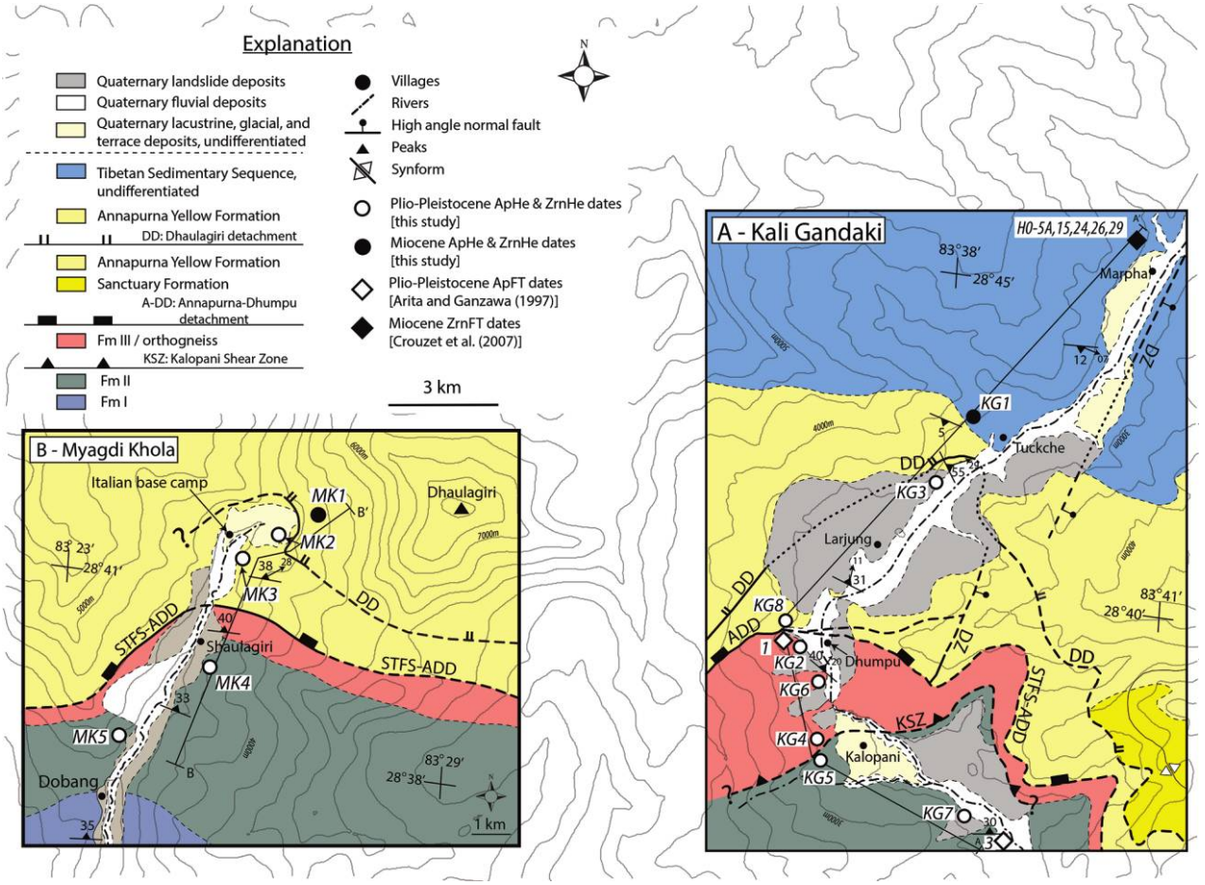

Figure 2. Structural and geologic maps of the Kali Gandaki (*A*) and Myagdi Khola (*B*) Valleys in central Nepal. Geologic relationships modified from Colchen et al. (1986), Vannay and Hodges (1996), Hurtado et al. (2001), Hurtado (2002), and Godin (2003). In the Kali Gandaki valley, zircon fission-track ages are from Crouzet et al. (2007), and apatite fission-track ages are from Arita and Ganzawa (1997); all zircon and apatite (U-Th)/He ages are from this study. Note that although Hurtado et al. (2001) mapped a small section in the corner between the immediate hanging wall of the Annapurna-Dhumpu Detachment and the footwall of the Dangardzong Fault as Formation II, further field and laboratory evaluation of samples from this wedge of material suggests that it is instead Annapurna Yellow Formation. Abbreviations: ADD = Annapurna-Dhumpu Detachment; ApFT = apatite fission-track; ApHe = apatite cooling; DD = Dhaulagiri Detachment; DZ = Dangardzong Fault; Fm = Formation; KSZ = Kalopani Shear Zone; STFS = South Tibetan Fault System; ZrnFT = zircon fission-track; ZrnHe = zircon cooling.

ture in the Kali Gandaki Valley, our research project was designed as an attempt to establish the extent of Quaternary deformation on low-angle, N-dipping faults in the transition zone, to explore the regional significance of these structures, and to set limits on the magnitude of Quaternary slip on these extensional structures. Our fieldwork also led us to the Myagdi Khola River valley to the west, a drainage that flows southward from the Dhaulagiri Massif and crosses the basal STFS a few kilometers southwest of the summit of Dhaulagiri I (figs. 1, 2*B*).

In both valleys, the basal STFS structure separates tectonostratigraphic packages that experienced distinctively different structural and metamorphic histories during the Cenozoic Era. In the Kali Gandaki Valley, the basal STFS structure is represented by the Miocene Annapurna Detachment first described by Brown and Nazarchuk (1993). The equivalent structure has been mapped farther east in the Annapurna Himalaya (fig. 1) as the Deorali Detachment in the Modi Khola Valley (Hodges et al. 1996) and the Chame Detachment in the Marsyandi Valley (Coleman 1996; Coleman and Hodges 1998). The footwall of the basal STFS detachment in all of these areas comprises upper-amphibiolite-facies pelitic, calc-silicate, and augen orthogneisses of the Greater Himalayan Sequence. These rocks are thought to represent the metamorphosed equivalents of Late Proterozoic–Cambrian strata originally deposited along the northern margin of Greater India, and they were intruded in places by Ordovician granites (Hodges 2000; Gehrels et al. 2011). In the Annapurna-Dhaulagiri Himalaya, the Greater Himalayan Sequence consists of a lowermost kyanite-bearing paragneiss (Formation I of Le Fort 1975). Overlying rocks are primarily calc-silicate gneisses with minor calcareous and psammatic schists and marbles (Formation II) and augen orthogneisses of Formation III.

The basal STFS hanging wall in the Annapurna-Dhaulagiri Himalaya comprises greenschist-facies to essentially unmetamorphosed carbonate and siliciclastic rocks of the Tibetan Sedimentary Sequence (e.g., Le Fort 1975). This succession represents nearly continuous Paleozoic to Eocene deposition on the northern Indian margin before the Indian-Eurasian collision (e.g., Bordet et al. 1971; Gaetani and Garzanti 1991; Godin 2003). In the Annapurna-Dhaulagiri region, the basal unit of the Tibetan Sedimentary Sequence is the Sanctuary Formation, a package of deformed, low-grade schists, sandstones, and limestones that crops out in the isolated hinges of fold nappes exposed east of the Kali Gandaki Valley (Pêcher 1978; Godin 2003). Overlying calcareous schists and minor interstratified siliciclastic rocks of the Annapurna Yellow Formation are the stratigraphically lowest Tibetan Sedimentary Sequence units exposed in our study areas. This package has also been referred to in the published literature as the Annapurna Formation, the Yellow Formation, or the Larjung Series (Bordet et al. 1971; Colchen et al. 1981; Godin 2003).

As is the case throughout the central Himalaya, the Greater Himalayan Sequence in the Annapurna and Dhaulagiri Ranges has been intruded by multiple generations of leucogranitic dikes and sills, most of which appear to be of Miocene age (Hodges et al. 1996). The extent to which these leucogranites persist structurally upward, across the STFS, is controversial. Several research teams have reported the occurrence of leucogranites (including the large Manaslu Pluton; fig. 1*D*) intruding the Tibetan Sedimentary Sequence in this region (e.g., Guillot et al. 1993, 1995; Hodges et al. 1996; Godin et al. 2001). By reinterpreting the Annapurna, Deorali, and Chame Detachments as structures distinctive from the STFS, as mapped elsewhere in the Himalaya, and mapping structurally higher normal faults as the basal STFS sensu stricto, Searle and Godin (2003) concluded that few or no leucogranites have intruded into the STFS hanging wall. In this contribution, we retain the traditional interpretation of the Annapurna Detachment (and its along-strike equivalents) as the basal STFS structure in the region (e.g., Brown and Nazarchuk 1993; Hodges et al. 1996; Hurtado et al. 2001). On the basis of that definition, we have documented numerous small dikes and sills of leucogranites above the STFS in the Kali Gandaki and Myagdi Khola Valleys, especially intruding stratigraphically lower units of the Annapurna Yellow Formation.

The youngest stratified units in the Kali Gandaki Valley are basin-fill lithologies and unconsolidated sediments of the Thakkhola Graben (Hurtado et al. 2001; Garzione et al. 2003). Deposited unconformably on Tibetan Sedimentary Sequence units, they range in age from upper Miocene to Quaternary. Only Quaternary strata of the basin-fill succession (ca. 35 ka and younger) are exposed in the area of figure 2*A*. As discussed further below, Quaternary basin-fill strata are of value in constraining the structural evolution of the upper Kali Gandaki drainage because they constrain the latest phase of slip on the Dangardzong Fault—the principal growth structure of the graben (figs. 1, 2*A*)—to between 150 and 17 ka, probably closer to the younger date (Hurtado et al. 2001). Very young strata that overlap the youngest deformational structures in the valley include extensive and probably diachronous landslide deposits (especially between the villages of Tukche and Dhumpu in fig. 2*A*), lacustrine sediments probably deposited when landslides temporarily dammed the Kali

Gandaki at various times in the recent past, and modern alluvium (Fort 2000; Hurtado et al. 2001).

The oldest penetrative fabrics in bedrock exposures above and below the basal STFS structure in this region are generally NW-SE-striking, moderately NE-dipping schistosities and associated NNE-NE-plunging lineations (Hodges et al. 1996; Vannay and Hodges 1996) that are synmetamorphic with respect to Miocene regional metamorphism. In the Kali Gandaki Valley, at the base of Formation III, older L-S fabrics were overprinted by noncoaxial strain fabrics related to the Kalopani Shear Zone of Vannay and Hodges (1996). On the basis of field examination of shear-sense indicators, this low-angle, N-dipping ductile shear zone was interpreted by Vannay and Hodges (1996) as having accommodated late-metamorphic reverse slip during the Miocene. We were unable to find good exposures of the appropriate structural levels in the Myagdi Khola Valley and thus could not confirm the extension of this structure to the west. (In fig. 2*B*, we designate the basal contact of Formation III with a dashed line.) However, a reverse-sense shear zone at the same structural position was mapped by Hodges et al. (1996) in the Modi Khola Valley, roughly 50 km east of the Kali Gandaki Valley, as the Modi Khola Shear Zone (fig. 1). In the Kali Gandaki Valley, Kalopani Shear Zone fabrics dominate the structure of Formation III to within 100 m of the Greater Himalayan Sequence–Tibetan Sedimentary Sequence contact, beyond which they are overprinted by noncoaxial fabrics related to the STFS (described below).

In contrast to the broadly uniform northeastward dip of compositional layering in the Greater Himalayan Sequence, bedding planes in the more weakly metamorphosed to unmetamorphosed units of the Tibetan Sedimentary Sequence above the basal STFS have been deformed into abundant mesoscopic and macroscopic folds. Godin et al. (1999) and Godin (2003) identified several generations of folds, mostly predating the STFS, and they inferred an Oligocene age for those structures.

Fold structures in the Tibetan Sedimentary Sequence are cut by a variety of high-angle, N- to NE-striking brittle faults, including the Dangardzong Fault. All are regarded as related to opening of the Thakkhola Graben (Hurtado et al. 2001; Godin 2003).

Structural Character of the Greater Himalayan Sequence–Tibetan Sedimentary Sequence Transition in the Kali Gandaki and Myagdi Khola Transects. In the Kali Gandaki Valley, the Annapurna Detachment is exposed low in a tributary catchment at 28°39′54″N, 83°35′06″E (fig. 2*A*). Footwall amphibolite-facies schists and gneisses, with deformed leucogranitic dikes and sills, contain a distinctive mylonitic fabric that is subparallel to the Greater Himalayan Sequence–Tibetan Sedimentary Sequence contact. S-C fabrics and stretching lineations in these rocks indicate normal-sense (hanging wall to the northeast) displacement during ductile deformation related to the Annapurna Detachment (Brown and Nazarchuk 1993; Godin et al. 1999). These noncoaxial fabrics persist upward into the Tibetan Sedimentary Sequence over a structural distance of about 100 m. A 5-m-thick zone of fault breccia oriented roughly parallel to the Annapurna Detachment marks the actual Greater Himalayan Sequence–Tibetan Sedimentary Sequence contact. While Brown and Nazarchuk (1993) and Godin et al. (1999) interpreted these brittle deformation features as related to the late stages of slip on the Annapurna Detachment, additional mapping by Hurtado et al. (2001) to the east, across the main Kali Gandaki Valley, showed that the prototypical exposure of the Annapurna Detachment in the tributary valley was, in fact, a segment of the detachment that had been reactivated as part of the later, brittle Dhumpu Detachment (fig. 2*A*). Inasmuch as this article focuses on the reactivated segment of the Annapurna Detachment, we refer to it here as the Annapurna-Dhumpu Detachment to avoid confusion.

In the Myagdi Khola Valley, the Greater Himalayan Sequence–Tibetan Sedimentary Sequence contact has a structural expression almost identical to that found in the Kali Gandaki Valley, so we are confident interpreting that contact as another exposure of the Annapurna-Dhumpu Detachment. It is particularly well exposed ca. 1 km north of Shaulagiri at 28°40′23.8″N, 83°25′08.5″E (fig. 2*B*). The immediate footwall there consists of highly sheared amphibolite-facies augen orthogneisses of the Greater Himalayan Sequence intruded by numerous leucogranitic dikes and sills that account for roughly 50% of outcrops by volume. Leucogranitic intrusions persist across the detachment into the lower-grade Tibetan Sedimentary Sequence calc-schists in the hanging wall. Ductile deformational fabrics, similar to those observed in the Kali Gandaki Valley, are also found in the footwall and hanging wall in the Myagdi Khola Valley (Larson and Godin 2009). Brittle deformation is evidenced by a narrow brecciated zone along the fault that dips ca. 20° N.

Structural Character of the Dhaulagiri Detachment. A second brittle detachment, previously described by Hurtado (2002) and linked to the slip on the STFS (STF3 of Hurtado 2002), has been identified structurally above the Annapurna-Dhumpu Detachment.

This "Dhaulagiri Detachment" is exposed on the west side of the Kali Gandaki Valley in a recently excavated road cut ~2.5 km north of the village of Larjung at 28°42′22.2″N, 83°38′02.9″E (fig. 3). It crops out as a discrete, shallow-dipping (293/8 NE) fault surface entirely within calcareous schist and psammite of the Annapurna Yellow Formation. Although the fault does not correspond to a lithologic boundary, it does mark a metamorphic discontinuity: greenschist-facies calcareous schists in the footwall against essentially unmetamorphosed phyllite and limestone in the hanging wall. Deformed Miocene leucogranitic dikes and sills are relatively abundant in the footwall but are absent from the hanging wall. Within the fault zone, both hanging-wall and footwall rocks are variably brecciated in a zone extending up to 200 m from the discrete fault. Footwall rocks display a strong brittle-ductile shear fabric (328/26) that dips subparallel to the fault plane, as well as a down-dip stretching lineation (030/17), but no definitive shear-sense indicators were found near the detachment in the Kali Gandaki Valley. Hanging-wall rocks are deformed into macroscale folds that can be traced along the high peaks of Dhaulagiri, Nilgiri, and Annapurna (e.g., Colchen et al. 1980). These folds are truncated by the Dhaulagiri Detachment, so the fault serves as a structural boundary as well, separating NE-dipping rocks in the immediate footwall from near-horizontal to shallowly S-dipping rocks in the immediate hanging wall (fig. 3). The detachment can be traced relatively easily for a short distance to the east into the Annapurna Range before it is buried by Quaternary landslides. Young landslide deposits

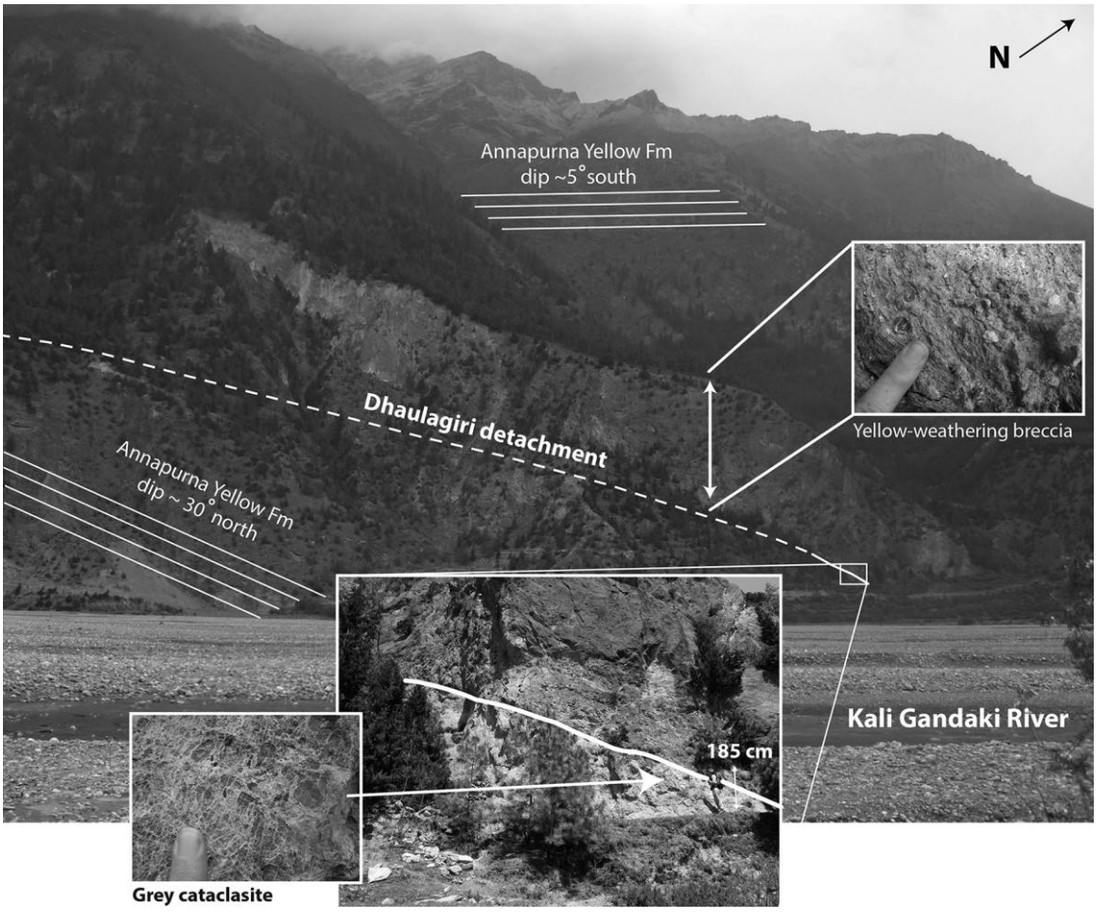

Figure 3. View of the Dhaulagiri Detachment in the Kali Gandaki River valley. Picture taken on the east side of the Kali Gandaki River ~1.5 km to the south of Tuckche, view to the ~N45°W. The fault crops out as a discrete structure with immediate footwall consisting of a grey cataclasite juxtaposed against hanging-wall yellow-weathering breccia. Hanging-wall strata are exposed in a cliff face ~200 m high above the fault, with compositional layering dipping at a much shallower angle than footwall rocks. Field assistant (~185 cm) for scale in close-up picture of the fault (bottom center).

obscure the region of probable intersection between the Dhaulagiri Detachment and the Dangardzong Fault, but seemingly offset traces of the latter structure to the north-northeast and the south-southwest suggest possible right-lateral separation of the Dangardzong Fault by the Dhaulagiri Detachment (fig. 2*A*). The trace of the Dhaulagiri Detachment dips subparallel to, but slightly shallower than, the dominant schistosity of the footwall rocks; on the basis of this relationship, the trace of the Dhaulagiri Detachment can be delineated trending toward, but not quite intersecting with, the Annapurna Detachment in the valley to the west of Dhumpu before the structure is lost in the snowfields high on the Dhaulagiri Massif (fig. 4).

In the Myagdi Khola Valley, the Dhaulagiri Detachment crops out as a discrete brittle-ductile shear zone (293/8 NE) in the glacial valley just north of the Italian base camp (28°42′01.3″N, 83°26′06.4″E; fig. 2*B*). As is the case in the Kali Gandaki Valley, the detachment crops out entirely within calcareous schists of the Annapurna Yellow Formation. Footwall rocks exhibit a strong schistosity (280/38) subparallel to the fault plane, while hanging-wall rocks display no detachment-related ductile fabrics. The fault is marked by a ca. 2-m-thick zone of fine breccia that dips ~20° NE. Subjacent footwall rocks contain well-developed ductile fabrics, and pervasive leucogranitic dikes in the footwall exhibit asymmetric extensional boudinage (fig. 5). These and other shear-sense indicators, as well as a ~062/28 stretching lineation, are consistent with hanging wall down-to-the-northeast (normal-sense) slip. Similar to the Kali Gandaki Valley, small, discordant leucogranite dikes are found throughout the footwall. Although several dikes can be traced into the fault zone in the Myagdi Khola Valley, all of these dikes display cataclastic deformation fabrics and clearly predate the Dhaulagiri Detachment.

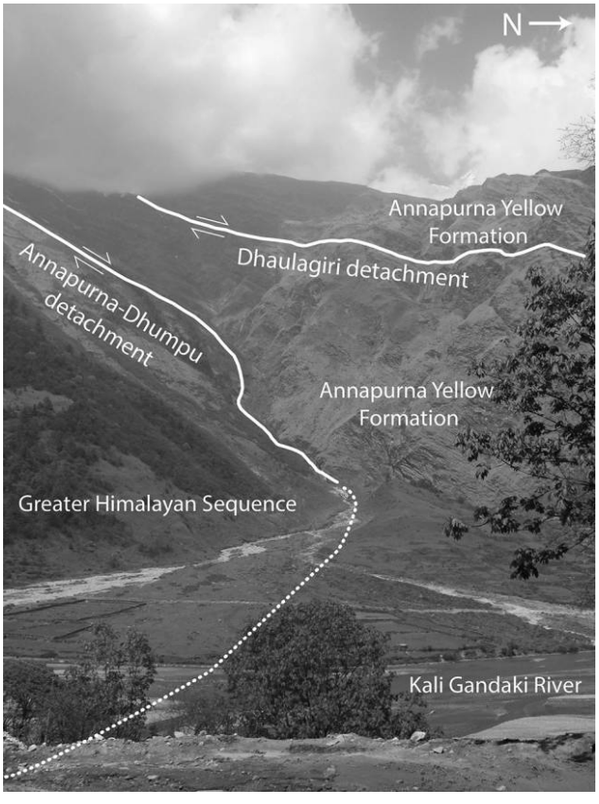

Figure 4. View of the Annapurna-Dhumpu and Dhaulagiri Detachments across the Kali Gandaki River to the immediate north of the village of Dhumpu. View is due west.

Thermochronologic Constraints on the Recent Slip History of the Annapurna-Dhumpu and Dhaulagiri Detachments

Hurtado et al. (2001) postulated that brittle slip on the Annapurna-Dhumpu Detachment took place during the Quaternary on the basis of mapped field relationships east of the Kali Gandaki Valley. The critical field relationship—truncation of the Dangadzong Fault by the Annapurna-Dhumpu Detachment—suggests that the detachment experienced at least minor slip after 150 ka, the maximum age of the youngest basin-fill units cut by the Dangadzong Fault (fig. 2*A*). In addition, possible offset of the Dangadzong Fault by the Dhaulagiri Detachment—something that is implied by the map relations but that we were unable to confirm because of poor exposure—would suggest similarly young displacement on the Dhaulagiri Detachment. Bedrock thermochronology provides a way to explore further the timing of latest slip on both structures. If significant Quaternary slip had occurred, we would expect the detachment traces to mark a discontinuity in hanging-wall and footwall cooling ages consistent with young, normal-sense deformation. Specifically, if such discontinuities exist, we would expect footwall cooling ages to be younger than hanging-wall cooling ages, and the footwall ages themselves would provide upper age bounds for significant fault slip.

Published zircon fission-track (ZrnFT) thermochronometric data from the Kali Gandaki Valley are indeed consistent with the Annapurna-Dhumpu Detachment, the Dhaulagiri Detachment, or both, having sustained significant Quaternary slip. Indic-

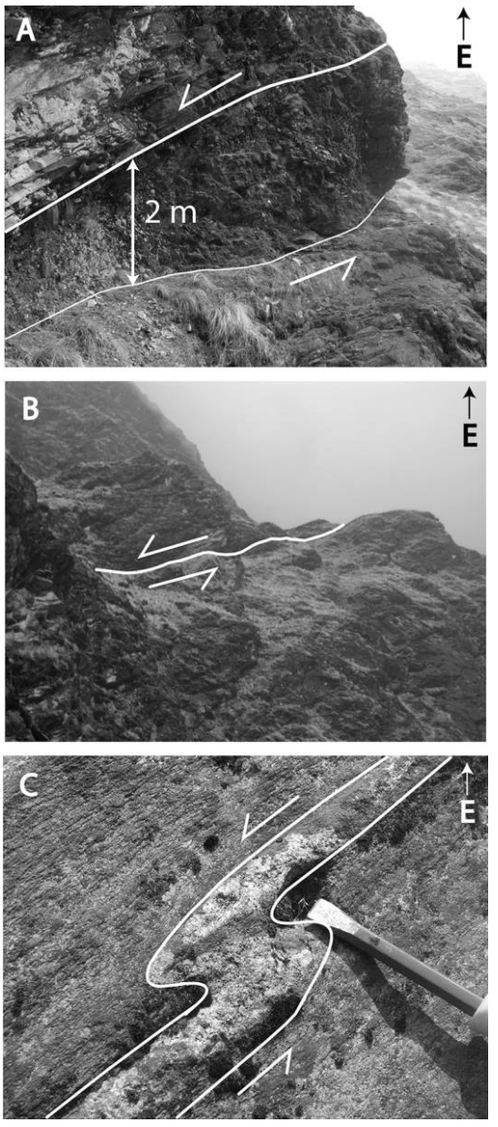

Figure 5. Details of the Dhaulagiri Detachment in the Myagdi Khola Valley. All photos taken due east. *A*, The Dhaulagiri Detachment crops out as a highly brecciated zone varying in thickness from ~2 to 8 m. *B*, The brecciated fault zone is defined by a recessive weathering horizon, allowing the fault to easily be traced toward the snowfields of Dhaulagiri to the east. *C*, Asymmetric extensional boudin in the footwall of the Dhaulagiri Detachment, showing top-to-the-north normal-sense displacement. Highly sheared leucogranite dikes are found at all structural levels within the footwall of the fault and are brittlely deformed within the brecciated zone. No leucogranite dikes are found in the hanging wall of the Dhaulagiri Detachment.

ative of the timing of cooling of samples below ca. 205°C (Bernet 2009), ZrnFT dates from the Annapurna-Dhumpu Detachment footwall are Pliocene or Quaternary (Arita and Ganzawa 1997), whereas dates from samples collected north of the trace of the detachment—and thus in its hanging wall—are Miocene (Crouzet et al. 2007; figs. 2*A*, 6). However, the geographic distribution of dated ZrnFT samples is such that the interpretation of the age differences as uniquely indicative of Quaternary movement on the Annapurna-Dhumpu Detachment is disputable. For example, the Miocene dates are for samples collected ~17 and ~6 km north of the trace of the Annapurna-Dhumpu and Dhaulagiri Detachments, respectively; thus, the observed ZrnFT discontinuity could result from slip on either or both detachments.

In order to better constrain the character of the cooling-age pattern, we determined (U-Th)/He cooling ages for zircons and apatites—referred to here as ZrnHe and ApHe dates, respectively—from a suite of samples from the Kali Gandaki and Myagdi Khola drainages (figs. 2, 6; tables S1a, S1b, available online). Below we discuss the results of this work in the context of three structural packages separated by the two detachments: the Dhaulagiri Detachment hanging wall, the Annapurna-Dhumpu Detachment hanging wall, and the Annapurna-Dhumpu Detachment footwall. (Note that the Annapurna-Dhumpu hanging-wall package also corresponds to the immediate footwall of the Dhaulagiri Detachment.)

Many low-temperature thermochronology studies are designed to shed light on bedrock exhumation histories and landscape evolutionary processes in tectonically active areas; optimal strategies for such studies typically involve the collection of samples along elevation profiles (Braun 2005). For this study, however, our goal was to constrain the relative cooling and exhumation histories of rock packages on either side of normal faults that dip at low angles (ca. 20°–25°) in a direction opposite to the steep topographic gradient of the Himalayan front. Because of this, we aimed to collect samples at similar elevations across the strike of the faults and the fall line of the Himalayan front. In a study area with more than 6000 m of local relief, the Kali Gandaki and Myagdi Khola drainages provided the best such opportunities. Although numerous samples were collected from all three packages in the two drainages, we were able to separate datable apatite from only 12 samples (seven from the Kali Gandaki Valley, five from the Myagdi Khola Valley) and datable zircon from only three samples, all collected in the Kali Gandaki Valley. Only two Kali Gandaki samples yielded both zircon and apatite (U-Th)/He dates. Samples were collected over total elevation ranges of roughly 800 m (2057–2846 m)

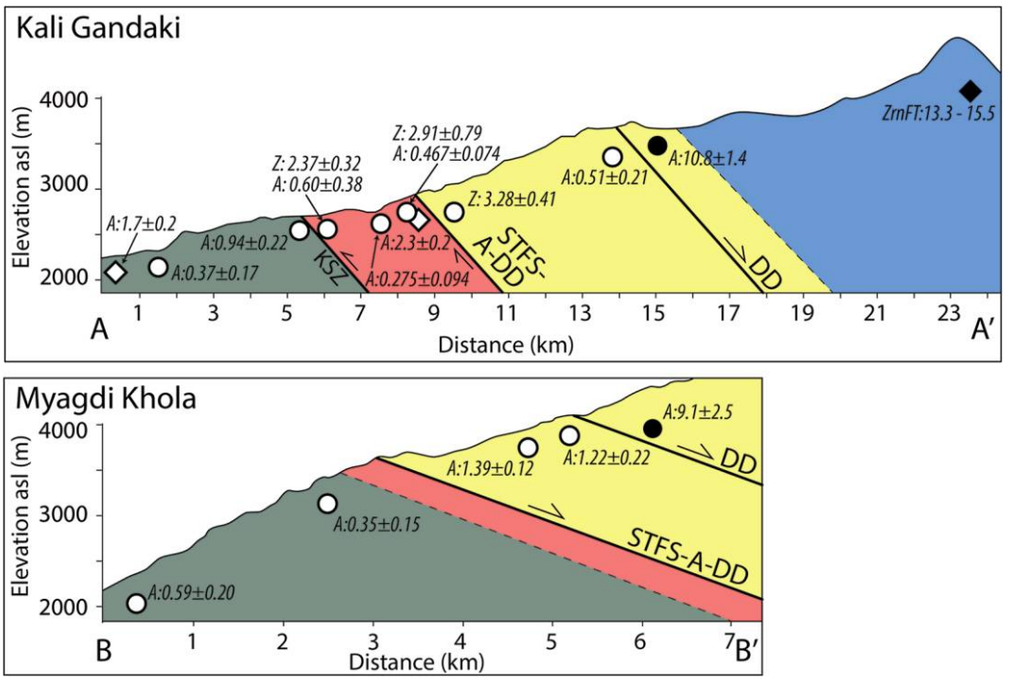

Figure 6. Simplified cross-sections along the Kali Gandaki (top: A-A′) and Myagdi Khola (bottom: B-B′) Valleys, showing the distribution of zircon fission-track and apatite and zircon (U-Th)/He dates. Section lines are indicated in figures 2*A* and 2*B*, respectively. Symbols and color scheme are the same as in figure 2. Note: vertical exaggeration is not the same for both cross sections. For new (U-Th/He) dates (circles; in Ma), apatite cooling ages are indicated with an "A" preceding the date, and zircon cooling ages are noted with a "Z" preceding the date. In the Kali Gandaki Valley, zircon fission-track ages are from Crouzet et al. (2007). Abbreviations: A-DD = Annapurna-Dhumpu Detachment; DD = Dhaulagiri Detachment; KSZ = Kalopani Shear Zone; STFS = South Tibetan Fault System.

and 1.2 km (2650–3854 m) along the Kali Gandaki and the Myagdi Khola, respectively (fig. 6).

The structurally lowest samples selected for dating were from rocks of the Greater Himalayan Sequence in the footwall of the Annapurna-Dhumpu Detachment, either Formation III augen orthogneiss or subjacent Formation II calc-silicate gneiss. Both zircon and apatite are relatively common accessories in Formation III orthogneiss, but euhedral, inclusion-free grains of both minerals (and especially zircon) are much less common. Only two Annapurna-Dhumpu footwall samples, both Formation III orthogneiss (KG-2 and KG-4), yielded both apatite and zircon suitable for dating.

Outcrops in the Annapurna-Dhumpu hanging wall are typically greenschist-facies calc-schists and impure marbles of the lower Annapurna Yellow Formation. Zircon suitable for (U-Th)/He dating was found in only one calc-schist sample at a relatively deep structural level in this intermediate package (KG-8). Apatite is somewhat more abundant in this package, but we identified datable euhedral or subhedral apatite in only one Kali Gandaki sample (KG-3) and two Myagdi Khola samples (MK-2 and MK-3).

Both zircon and apatite are relatively uncommon in the Annapurna Yellow Formation calc-schists and impure marbles of the Dhaulagiri hanging wall. In all of the samples from this structural package that we examined petrographically, the grain size of zircon was too small for analysis. Most observed apatites contained high-birefringence inclusions (possibly zircon or monazite) that made them unsuitable for (U-Th)/He dating. Only one sample from each drainage—KG-1 from the Kali Gandaki and MK-1 from the Myagdi Khola—yielded apatites that were sufficiently large, euhedral, and optically free of inclusions. Analytical methods are discussed in detail in the appendix, available online.

Results. A number of previous studies of Greater Himalayan Sequence samples from Nepal have yielded Pliocene–Quaternary fission-track and (U-Th)/He dates (e.g., Blythe et al. 2007; Robert et al. 2009; Herman et al. 2010; Nadin and Martin 2012; Streule et al. 2012; McDermott et al. 2013), and our samples from the Annapurna-Dhumpu footwall in

both the Kali Gandaki and Myagdi Khola Valleys corroborate those results (figs. 2, 6; tables S1a, S1b). Weighted-mean ZrnHe dates from this structural package were statistically indistinguishable: 2.37 ± 0.32 and 2.91 ± 0.79 Ma. ApHe dates were all Pleistocene, ranging from 0.275 ± 0.094 to 0.94 ± 0.22 Ma. Despite the narrow range, the observed dispersion of weighted-mean dates is significantly greater than would be expected from analytical imprecision alone (even after MSWD correction). The dates do not correlate well with elevation, as is evident because the collection localities for the youngest and oldest samples differed in elevation by only about 140 m. Likewise, there is no significant positive correlation between crystal size or effective uranium contents of the apatites that might help to explain the dispersion as a consequence of variable diffusion domain size or radiation damage (cf. Shuster et al. 2006). Other plausible sources for the variation are U+Th zoning in the apatites (Meesters and Dunai 2002; Hourigan et al. 2005), the effects of alpha implantation from neighboring high-U+Th minerals in the sample (Spiegel et al. 2009; Gautheron et al. 2012), or the effects of high-U+Th inclusions that were not detected during microscopic examination of the grains before analysis.

Samples from the Annapurna-Dhumpu hanging wall have ZrnHe and ApHe dates that are very slightly older, on average, than those for the footwall. Zircon from sample KG-8 yielded a weighted-mean date of 3.28 ± 0.41 Ma, while apatites from three samples yielded weighted-mean dates of 1.39 ± 0.12, 1.22 ± 0.22, and 0.51 ± 0.21 Ma. The two older ApHe dates are from elevations in the Myagdi Khola drainage higher than that for the younger date from the Kali Gandaki, suggesting that the difference may be related to regional topographic variations. However, within a single transect and at similar elevations, there appears to be no statistically significant difference between ZrnHe and ApHe dates from the Annapurna-Dhumpu footwall and those from the hanging wall, given our estimates of analytical precision. For example, apatites from KG-4 and KG-3, collected on opposite sides of the Annapurna-Dhumpu Detachment trace in the Kali Gandaki drainage, yielded statistically indistinguishable (U-Th)/He dates of 0.60 ± 0.38 and 0.51 ± 0.21 Ma.

In contrast, the available ApHe data from the Dhaulagiri hanging wall—though sparse—indicate a distinctive low-temperature cooling history for that structural package that is consistent with the previously published ZrnFT data of Crouzet et al. (2007). Samples from each drainage (KG-1 and MK-1) yielded statistically indistinguishable dates of 10.8 ± 1.4 and 9.1 ± 2.5 Ma. Regardless of the relatively large uncertainties on these dates—a consequence of their low uranium contents—both dates are roughly an order of magnitude older than dates for deeper structural levels.

Modeled Pleistocene Exhumation Histories. The simplest interpretation of thermochronologic dates is that they represent the time in the past at which minerals cooled through their nominal closure temperatures (the temperature thought to correspond to the determined cooling age of a sample). Dodson (1973) showed how these temperatures could be quantified, under the assumption of a constant cooling rate, as a function of cooling rate, effective diffusion dimension (typically crystal size for (U-Th)/He thermochronometers), and laboratory constraints on the temperature dependence of daughter-element diffusivity. For rapidly exhuming regions such as the Himalaya, the dependence of closure temperature on cooling rate is weak (Reiners and Brandon (2006). The crystal sizes of the minerals we dated—coupled with kinetic parameters for ^{4}He diffusion published by Farley (2000) and Reiners et al. (2004)—suggest nominal bulk closure temperatures of ca. 70° and 185°C for apatite and zircon, respectively. Assuming that cooling of the samples through those temperatures is a manifestation of advection of rocks upward toward the surface through a dynamic geothermal gradient, the dates can be used to calculate rates of exhumation since closure (Willet and Brandon 2013).

The size and spatial distribution of our (U-Th)/He data set do not lend themselves well to the kind of numerical, multidimensional thermal-kinematic modeling that is being used with increasing frequency to extract exhumation rates from thermochronometric dates (e.g., Whipp et al. 2007; Herman et al. 2010), so we present below the results of simple one-dimensional analytical models based on approaches outlined by Willett and Brandon (2013; see also Moore and England 2001). Although a one-dimensional approach simplifies the examination of denudation to a predominantly vertical component, previous work in the Himalaya has shown that lateral variations in the geothermal gradient are of relatively limited importance for (U-Th)/He and fission-track thermochronometric systems in regions experiencing high erosion rates (Whipp et al. 2007, 2009; Thiede and Ehlers 2013). Our one-dimensional calculations—which we refer to as "transient models"—used the "evolving half-space" approach of Willett and Brandon (2013), which takes both heat advection and conduction into account and features a constantly evolving geotherm. That method requires input of the modern geothermal gradient (presumed to be linear in the near-surface region), a mean elevation, the mean surface tem-

perature at that elevation, and an age for the onset of the most recent phase of exhumation responsible for bringing dated samples to the surface.

Geothermal gradients along the Himalayan front are typically high. Derry et al. (2009). estimated a very high value of 75°C/km based on work in central Nepal, including our study area. This estimate is based on fluid inclusion work done on samples collected from structural levels corresponding to the Annapurna-Dhumpu footwall as defined in this study, and the high geothermal gradient is consistent with thermochronologic evidence for rapid exhumation at this structural level. It is unclear whether such a high geothermal gradient also applies to regions corresponding to outcrop areas of the Annapurna-Dhumpu and Dhaulagiri hanging walls. For illustrative purposes, we compare in table 1 results based on two geothermal gradient assumptions: one the empirical value of 75°C/km and the other the much lower value of 35°C/km.

While the elevations at which samples were collected were measured, it is important to account for the local effects of topography on the evolving thermal field during exhumation, and this is most effectively done by adjusting the elevations to a local "mean" elevation (Braun 2002). We did so by following the approach outlined by Willett and Brandon (2013), which involved computing a mean elevation for each sample by averaging over a circular area, centered on the sampling site, with a radius of approximately 2.5 km. We assumed a mean surface temperature at all sampling locations of 5°C.

For the Dhaulagiri Detachment hanging-wall samples, which yielded Late Miocene ApHe dates, we assumed an onset for the most recent exhumation phase at 20 Ma, consistent with the findings of previous higher-temperature thermochronology studies in the area (Vannay and Hodges 1996). For samples from farther south and at deeper structural levels, the same assumption is likely to be incorrect because of evidence in the region for accelerated exhumation since the Pliocene (Huntington and Hodges 2006; Huntington et al. 2006; Whipp et al. 2007; McDermott et al. 2013), and we instead assumed onset for the most recent exhumation phase at 4 Ma (just slightly older than the oldest ZrnHe date).

Transient models based on ApHe data for the Dhaulagiri hanging wall (table 1) indicate low average exhumation rates ($\dot{E}$) of 0.041–0.058 km/Ma, assuming a modern geothermal gradient (G_{mod}) of 75°C/km, or 0.13–0.16 km/Ma, assuming G_{mod} = 35°C/km. Such rates imply that the Péclet number for heat transport—the ratio of heat advection to heat diffusion—was low over most of the exhu-

Table 1. Modeled Exhumation Histories

	Transient models (G_{mod} = 75°C/km)			Transient models (G_{mod} = 35°C/km)		
Structural unit	$\dot{E}$ (km/Ma)	E_Q (km)	ΔE_Q (km)	$\dot{E}$ (km/Ma)	E_Q (km)	ΔE_Q (km)
Dhaulagiri hanging wall:[a]						
ApHe models (based on 7 dates from 2 samples)	.041–.058	.10–.15	...	.13–.16	.34–.41	...
Annapurna-Dhumpu hanging wall:[b]						
ZrnHe model (based on 3 dates from 1 sample)	.83	2.1	...	4.8	12	...
ApHe models (based on 12 dates from 3 samples)	.52–1.7	1.3–4.4	1.2–4.3	1.5–5.6	3.9–14	3.5–14
Annapurna-Dhumpu footwall:[b]						
ZrnHe models (based on 6 dates from 2 samples)	1.1–1.3	2.8–3.4	...	9.0–13	23–34	...
ApHe models (based on 26 dates from 7 samples)	1.1–2.6	2.8–6.7	2.7–6.6	4.4–31	11–80	11–80

Note. Transient solutions (assuming changing geothermal gradients due to heat advection) are calculated with the approaches of Willett and Brandon (2013). $\dot{E}$ = exhumation rate; E_Q = estimated net exhumation since the base of the Quaternary Period (2.58 Ma; Gibbard et al. 2010), assuming constant $\dot{E}$; ΔE_Q = estimate of net differential Quaternary exhumation between the structural unit and the Dhaulagiri Detachment hanging wall. Helium diffusion kinetic parameters are from Farley (2000) for ApHe and from Reiners et al. (2004) for ZrnHe. Modeling assumed two different values for the modern geothermal gradient (G_{mod}): the 75°C/km value estimated for this area by Derry et al. (2009) and a low value of 35°C/km for illustrative purposes. The surface temperature was assumed in all cases to be 5°C, and sample elevations above the mean elevation in the area were estimated with equation (2) of Willett and Brandon (2013). ApHe = apatite cooling age; ZrnHe = zircon cooling age.

[a] Onset of exhumation event assumed to be 4 Ma.

[b] Onset of exhumation event assumed to be 20 Ma.

mation interval. For purposes of illustration, we have defined a quantity E_Q as the amount of exhumation implied by an average exhumation rate since the beginning of the Quaternary Period at 2.58 Ma (Gibbard et al. 2010). For the Dhaulagiri hanging wall, the assumption of exhumation at a constant rate since Late Miocene ApHe closure implies E_Q = 0.10–0.15 or 0.34–0.41 km, depending on which G_{mod} value we choose. Although exhumation rates for this structural package may have increased since the Late Pliocene, they cannot have increased much; otherwise, the measured ApHe dates for this structural package would be much younger, given the likely shallow depth of the ApHe closure isotherm.

Transient models for the Annapurna-Dhumpu hanging wall and footwall suggest exhumation rates that were more than an order of magnitude faster than those of the Dhaulagiri hanging wall using a single value for G_{mod} (the same G_{mod} value for rock packages on both sides of the fault), or at least three times faster even if we assume a G_{mod} for the Annapurna-Dhumpu hanging wall drastically lower (35°C/km) than that for its footwall (75°C/km; table 1). Only one ZrnHe date from the Annapurna-Dhumpu hanging wall could be modeled, but its estimated exhumation rate (0.83 or 4.8 km/yr for the higher and lower G_{mod} values, respectively) are within the ranges of values modeled for the ApHe dates from the same package, implying that the data are collectively consistent with exhumation at a more or less constant rate since ZrnHe closure at ca. 3.3 Ma. The same is broadly true for transient Annapurna-Dhumpu footwall models, with $\dot{E}$ values calculated from ZrnHe dates ranging from 1.1 to 1.3 km/Ma (or 9.0–13 km/Ma for the lower assumed geothermal gradient) and those calculated from ApHe dates ranging from 1.1 to 2.6 km/Ma (or 4.4–31 km/Ma for G_{mod} = 35°C/km). For the most part, calculated E_Q values for the Annapurna-Dhumpu footwall samples are higher than those for hanging-wall samples, consistent with limited differential slip across this detachment during the Pleistocene. Table 1 also shows calculated values for ΔE_Q, the difference, based on ApHe dates, between E_Q values for the Dhaulagiri hanging wall and those for the two other structural packages. (A similar calculation based on ZrnHe dates was not possible because we found no datable zircon in the Dhaulagiri hanging wall.) The transient models based on G_{mod} = 75°C/km suggest 1.2–4.3 km more exhumation of the Annapurna-Dhumpu hanging wall and 2.7–6.6 km more exhumation of the Annapurna-Dhumpu footwall, as compared to the Dhaulagiri hanging wall, during the Pleistocene. Using G_{mod} = 35°C/km for the Dhaulagiri hanging wall and G_{mod} = 75°C/km for all footwall units, which minimizes the apparent differential exhumation above and below the Dhaulagiri Detachment, still leads to a minimum ΔE_Q of at least ca. 0.89 km.

Sensitivity Analysis of Models and Comparisons with Other Average Exhumation Rate Estimates. The value of modeling exercises like these is always limited by our confidence in the assumptions behind them. Our assumption regarding different initiation ages of the latest exhumation event in different structural packages—20 Ma for the Dhaulagiri hanging wall and 4 Ma for the Annapurna-Dhumpu hanging wall and footwall—has an effect on the magnitude of modeled $\dot{E}$, E_Q, and ΔE_Q values. However, changing the initiation age to a uniform value of 20 Ma for all structural packages would lead to only about a 3% reduction in modeled $\dot{E}$. Changes of that magnitude would not influence the essential finding that Quaternary exhumation rates were at least an order of magnitude lower in the Dhaulagiri hanging wall than in structurally lower rock packages.

Exhumation rates at all structural levels are highly sensitive to the assumed value of G_{mod}. For comparative purposes in table 1, we have presented the results of modeling assuming both the high value preferred for this region by Derry et al. (2009) and a much lower value more in keeping with typical continental values (35°C/km). The lower value of G_{mod} results in large increases in modeled $\dot{E}$ for all structural levels, but the dramatic difference between Pleistocene exhumation rates of the Dhaulagiri hanging wall and those of deeper structural packages remains. The same is true even if we assume the 35°C/km value for the hanging wall and 75°C/km for deeper structural levels exposed south of the trace of the Dhaulagiri Detachment. Our transient models carry with them the implicit assumption that conduction and advection were the only operative modes of heat transfer. In detail this is certainly incorrect, insofar as there is abundant evidence for hydrothermal activity in the lower Kali Gandaki and Myagdi Khola Valleys. As noted by Derry et al. (2009), hydrothermal fluid circulation has the potential to influence the closure behavior of low-temperature thermochronometers and could compromise efforts to interpret closure ages as indicative of exhumation rates. Whipp and Ehlers (2007) explored this effect explicitly for the southern flank of the Annapurna Range, using a three-dimensional, coupled hydrologic and thermokinematic model. They estimated that models failing to account for fluid advection of heat could underestimate exhumation rates by on the order of 200%. However, hydrothermal activity is highly localized in the Himalaya. Within our field area, modern

hydrothermal deposits of significant extent have been described only near Tukche, in the immediate hanging wall of the Dhaulagiri Detachment (Hurtado 2002). The only one of our samples collected in this area (KG1) also yielded the oldest ApHe date of our entire data set (10.8 ± 1.4 Ma). Heating of this sample by young hydrothermal fluids, if it happened at all, did not affect its helium isotopic systematics enough to reduce the discrepancy between its apparent age and those of apatites from deeper structural levels. Most modern and ancient hot-spring deposits in the two valleys are found near the trace of the Main Central Thrust System, more than 15 km south of our southernmost collection localities.

Previous efforts to estimate Late Miocene–Pleistocene exhumation rates in the Annapurna Range from thermochronometric data have involved direct interpretations of apparent age-elevation profiles (Huntington and Hodges 2006; Huntington et al. 2006; Blythe et al. 2007), modeling of detrital mineral cooling ages from samples of modern river deposits (Brewer et al. 2003, 2006; Ruhl and Hodges 2005; Huntington and Hodges 2006), and one-, two-, and three-dimensional thermokinematic modeling of distributed data, particularly apatite and ZrnFT dates (Burbank et al. 2003; Huntington et al. 2006; Whipp and Ehlers 2007; Whipp et al. 2007; Nadin and Martin 2012). All of these estimates are based on minerals in bedrock or detrital samples from Greater Himalayan Sequence lithologies collected from structural levels most comparable to the collection sites of the Annapurna-Dhumpu footwall samples we studied. The data from higher-temperature thermochronometers—for example, muscovite $^{40}Ar/^{39}Ar$, with a nominal closure temperature range of 400°–500°C (Harrison et al. 2009)—indicate Late Miocene–Early Pliocene exhumation at rates of 0.57–2.3 km/Ma. Fission-track and (U-Th)/He data from previous studies have been interpreted as indicative of Late Pliocene–Quaternary exhumation rates of 0.5–12 km/Ma, but most estimates are in the lower end of that range (≤5 km/Ma). Our transient-model results for similar structural levels (1.1–2.6 km/Ma; table 1) are comparable to those obtained in the course of earlier studies.

Interpretation of Average Exhumation Rate Estimates. Exhumation rates modeled from low-temperature thermochronometric data are frequently interpreted as bedrock erosion rates, and abrupt changes in the trend of dates obtained with a particular thermochronometer and collection elevation can be interpreted as indicative of abrupt changes in erosion rate and/or topographic relief at a particular time over a relatively broad area (e.g., Braun 2005). We do not favor such an interpretation of the most dramatic such change in our data set—from Late Pliocene–Pleistocene ZrnHe and ApHe dates south of the trace of the Dhaulagiri Detachment to Late Miocene dates to the north—for a variety of reasons. First, although it is true that the sampling elevations are higher for the two rocks yielding the Late Miocene ApHe dates, the dates for all samples do not increase systematically with sampling elevation. For example, the 9.1 Ma ApHe date (MK1) was obtained for a sample collected about 1 km higher than the sample that yielded a 10.8 Ma date (KG1). Furthermore, three samples from the Modi Khola Valley that were collected at higher elevations than KG1 (MK2, MK3, and MK4) yielded ApHe dates an order of magnitude younger. Second, the ca. 9–10 Ma difference between the ApHe closure dates for the Dhaulagiri hanging wall and those for deeper structural levels is impossible to reconcile with the total elevation difference across which all samples were collected. If we extrapolate our lowest estimate for the exhumation rate of the deeper samples (0.52 km/Ma) backward in time to the beginning of the Pleistocene, the rocks from which the Late Miocene dates were obtained would be completely eroded away. Finally, and most convincing from our perspective, the transition from Pleistocene cooling dates to Late Miocene cooling dates coincides with the surface trace of the Dhaulagiri Detachment (fig. 6).

The low exhumation rates indicated by the northernmost of our samples could also be the result of well-documented decrease in rainfall from south to north across the southern flank of the Himalaya. However, all of our samples are from elevations experiencing between about 2 and 4 m/yr of predominantly monsoonal precipitation (Bookhagen and Burbank 2010), and similar variations apparently have not disrupted cooling-age patterns just to the east of our study area in the Annapurna Range (Burbank et al. 2003).

We regard the interpretation that the transition in cooling dates across the Dhaulagiri Detachment is a direct consequence of detachment slip as more likely than any interpretation involving only a change in erosional-exhumation rate. If correct, our interpretation indicates that the Dhaulagiri Detachment has been active in the Pleistocene, an observation consistent with the structure's apparent offset of the Dangardzong Fault, which experienced young (but pre–17.2 ka) Quaternary slip (Hurtado et al. 2001). The minimum age of latest slip is poorly constrained, but the fault does not appear to cut Holocene fluvial and landslide deposits in the Kali Gandaki Valley. The fact that Dhaulagiri footwall ApHe dates are much younger than hanging-wall ApHe dates is consistent with

normal-sense displacement, with fault slip responsible for tectonic denudation of underlying rocks. One reasonable inference is that the differential Quaternary exhumation across the detachment—at minimum, roughly 0.89 km, and perhaps as much as 14 km in the extreme—represents the cumulative throw. Assuming a planar geometry for the detachment at depth, a ca. 25° dip (based on field observations in the Kali Gandaki Valley), and a purely down-dip displacement vector, this inference permits estimates of Quaternary displacement between ca. 2 and 33 km, although we think that a more realistic range is ca. 3–10 km.

The amount of Quaternary displacement on the previously recognized Annapurna-Dhumpu Detachment is unclear. Comparison of mean E_Q estimates for hanging-wall and footwall samples suggest the potential for up to a few kilometers of throw, but the broad overlap of hanging-wall and footwall E_Q values (due largely to the ApHe dates for sample KG3) could be interpreted to indicate no significant differential exhumation. Better thermochronologic constraints on the Annapurna-Dhumpu hanging-wall cooling history are needed to further evaluate the magnitude of slip on this structurally deeper Quaternary structure and its tectonic significance relative to the structurally higher Dhaulagiri Detachment.

It may seem incongruous to some readers that the summits of two of the highest mountains in the world—Dhaulagiri and Annapurna—expose rocks in the hanging wall of Quaternary low-angle normal faults with significant displacement. However, the overall topographic profile of the Himalaya in the study area reflects dramatic south-to-north variations in the precipitation pattern as well as the evolving geometry of shortening structures in the Himalayan orogenic wedge, which still absorbs upward of 2 cm/yr of India-Eurasia convergence (Ader et al. 2012). Considerable evidence exists in central Nepal for an active ramp in the basal thrust of the wedge ("the Himalayan sole thrust"), as well as out-of-sequence shortening in the central region of the wedge, either on blind duplex structures at depth or on surface-breaking thrust faults (Pandey et al. 1995; Cattin and Avouac 2000; Wobus et al. 2005). Quaternary activity on these structures has passively elevated the entire study area, including both hanging walls and footwalls of the studied detachments. The fact that the summits of Dhaulagiri and Annapurna remain higher than rocks exposed in the footwalls of the Dhaulagiri and Annapurna-Dhumpu implies that tectonic denudation related to the detachments has not been sufficiently high to counter broader uplift trends related to orogenic wedge evolution and that erosion rates on the Dhaulagiri and Annapurna Massifs have been less than rates farther south, where monsoonal precipitation is higher.

Regional Significance of Quaternary Detachments

The new thermochronologic data presented here, coupled with previous thermochronologic and structural data from central Nepal, indicate that N-S-directed extension near the crest of the range played a role in both the Miocene and the Quaternary tectonic evolution of the Annapurna and Dhaulagiri Himalaya. Whether this extension has occurred continuously or episodically over the past 20 m.yr. remains unknown.

If Quaternary slip on the Dhaulagiri Detachment is responsible for a major disruption of bedrock cooling-age patterns for low-temperature thermochronometers in the study area, as inferred here, we might argue that such a structure would be regional in extent. In fact, several candidate correlative or related structures have been mapped to the north, east, and west of our field site (Nakata 1989; Hodges et al. 1996; Coleman 1996; Searle and Godin 2003; Styron et al. 2011; Murphy et al. 2014).

To the north, but still within the Kali Gandaki drainage, Godin (2003) mapped the Quaternary Lupra normal fault (fig. 1), which has a strike similar to that of the Dhaulagiri Detachment but a substantially steeper dip. While this structure may be related to the detachment in some way, it also exhibits geologic relationships consistent with genetic relationship to Thakkhola Graben development.

To the east across the Annapurna Himalaya, previous work established the presence of multiple generations of top-to-the-north, low-angle extensional structures, subparallel to but structurally higher than the STFS. Historically, these structures have been considered part of the STFS, and, because there have been no age constraints on those structures, many of them were presumed to be of Miocene age, perhaps only slightly younger than the basal STFS detachments (e.g., Hodges et al. 1996; Searle et al. 2003). However, several of those faults are similar in character to the Dhaulagiri Detachment and may have accommodated Quaternary deformation. One of these structures, in particular, the Machhapuchhare Detachment (fig. 1), may be a candidate for the eastward extension of the Dhaulagiri Detachment. Exposed in the Modi Khola drainage, ~35 km to the east of the study area, this structure has been mapped as a low-angle, (~25°) WNW-striking, brittle-ductile shear zone (Hodges et al. 1996). Like the Dhaulagiri Detachment, it strikes subparallel to, but structurally above, the basal

STFS in the Modi Khola drainage. Footwall kinematic indicators are consistent with ductile, top-to-the-north (normal-sense) displacement, but no indicators were found that directly constrain the kinematics of brittle shearing. The Machhapuchhare Detachment marks a sharp metamorphic discontinuity, placing greenschist-facies Sanctuary Formation rocks on amphibolite-facies rocks of the Annapurna Yellow Formation. The fault serves as the truncating boundary for macroscale folds that dominate the hanging wall and for all leucogranite dikes and sills that crosscut the footwall. Attempts to trace the structure to the west toward the Kali Gandaki Valley using satellite imagery have been unsuccessful. We believe that this is largely because the fault strikes parallel to the general fall line of topography, dips only shallowly to the north, and juxtaposes rocks with similar outcrop characteristics. However, on the basis of inspection of satellite imagery, Hurtado (2002) identified a short segment of a fault that we now interpret as a continuation of the Dhaulagiri Detachment about 10 km to the east of the Kali Gandaki River valley. That segment truncates the macroscale folds in the hanging wall and juxtaposes rocks of the Sanctuary Formation on Annapurna Yellow Formation rocks. The fact that this is the same stratigraphic relationship documented in the Modi Khola Valley on the Machhapuchhare Detachment (Hodges et al. 1996) supports a correlation of the Dhaulagiri and Machhapuchhare Detachments. Several younger subparallel normal faults, such as the Hiunchuli Detachment, were also mapped in the hanging wall of the Machhapuchhare Detachment by Hodges et al. (1996). These were originally interpreted by Hodges et al. (1996) as imbricate hanging-wall splays off the Machhapuchhare Detachment, but the actual fault intersections that would have confirmed that interpretation were not observed. The timing of displacement on the Machhapuchhare Detachment is currently constrained only by the fact that it cuts leucogranite bodies with crystallization ages (constrained by U-Pb geochronology) as young as 18.5 Ma (Hodges et al. 1996). No available data preclude a Quaternary age for brittle deformation on this structure or its correlation with the Dhaulagiri Detachment.

Previous workers have proposed correlation of the Machhapuchhare Detachment with the Phu Detachment in the Marsyandi Valley farther to the east (Searle and Godin 2003), and indeed, the Phu Detachment exhibits similar structural characteristics. However, the Phu Detachment is demonstrably folded and therefore seems unlikely to be Quaternary in age (Godin et al. 2006). Blythe et al. (2007) examined a suite of ApHe and apatite fission-track (ApFT) and ZrnFT ages from the footwall region of the Phu Detachment in the Marsyandi Valley and found cooling ages ranging from 0.3 to 0.9 Ma (ApHe), from 0 to 3.8 Ma (ApFT), and from 0.8 to 1.9 Ma (ZrnFT), suggestive of an increase in exhumation rate as recently as ~1 Ma. Although this change in exhumation is unlikely to have been the result of slip on the folded Phu Detachment, we cannot rule out that it was related to tectonic denudation on a Quaternary detachment, and thus, correlative structures to the Dhaulagiri Detachment may also occur in the Marsyandi region.

Because of poor infrastructure and political sensitivity until very recently, the region immediately west of the Myagdi Khola Valley has not been extensively mapped. On the basis of an analysis of aerial photographs, Nakata (1989) mapped a number of young (Late Pleistocene–Holocene) fault structures in western Nepal. Of particular interest is ca. N50°W-striking structure exposed about 30 km west-southwest of the Dhaulagiri Massif that Nakata (1989) referred to as the Dhaulagiri Southwest Fault. A recent, detailed field study along part of this structure by Murphy et al. (2014) showed it to be one of a series of recently active faults that have been postulated to extend dextral slip on the Karakoram Fault System—a major tectonic feature that effectively defines the extreme southwestern margin of the Tibetan Plateau—southeastward to the Himalayan front at the approximate longitude of Dhaulagiri (Styron et al. 2011; Murphy et al. 2014). Referred to as the Western Nepal Fault System by Murphy and colleagues, this ca. 350-km-long system shows evidence of oblique slip—with a N- to NE-directed normal component and a dextral component. The dextral component of slip along most segments of the Western Nepal Fault System appears to be greater than the normal component, on the basis of Late Pleistocene offset markers (Silver 2012; Murphy et al. 2014). However, the Dhaulagiri Southwest Fault, while having a steeper northward dip and cutting exclusively through Greater Himalayan Sequence rocks, has the appropriate orientation and trace to suggest a possible correlation with either the Annapurna-Dhumpu Detachment (as suggested by Hurtado et al. 2001) or the Dhaulagiri Detachment. We tentatively favor a correlation with the Dhaulagiri Detachment, but satellite imagery for the region between the upper Myagdi Khola Valley and the closest place where the trace of the Dhaulagiri Southwest Fault is obvious (a distance of about 20 km) show no clear geomorphic signature of a connection. In our experience, this is not particularly discouraging, because the traces of low- and moderate-angle faults of this orientation are notoriously difficult to follow

in satellite imagery of the Himalaya. One observation that may argue against a correlation is that Silver (2012) found evidence of only a few tens of meters of normal slip on the Dhaulagiri Southwest Fault and regards this structure as having predominately strike-slip offset. However, all of the kinematic indicators leading to that conclusion are based on offsets of geomorphic features and moraine deposits no older than the end of the Last Glacial Maximum (ca. 19 ka). There is no direct evidence for slip on the Dhaulagiri Detachment in the Myagdi Khola or Kali Gandaki Valleys over the past 19 kyr, although the data available do not prohibit slip that young. It is plausible that there was an older, predominantly normal-sense slip history on the Dhaulagiri Southwest Fault that has been overprinted by very young dextral slip on the Western Nepal Fault System. To the best of our knowledge, systematic low-temperature thermochronologic studies have not been conducted across the trace of the Western Nepal Fault System, but they could provide important information regarding the viability of a correlation with the Dhaulagiri Detachment.

Recent work in the Nyalam region of south-central Tibet documented evidence for Plio-Pleistocene, top-to-the-north displacement on a low-angle detachment at approximately the same structural level as the detachments described here (McDermott et al. 2013). As is the case in the Kali Gandaki and Myagdi Khola areas, the structure near Nyalam also disrupts the local pattern of cooling ages for (U-Th)/He thermochronometers. The specific relationship between Quaternary normal faulting in Nyalam and that in the Annapurna-Dhaulagiri Himalaya is unknown at this time, but the current work adds to the growing evidence for N-directed normal faulting near the crest of the range since Miocene time.

The recognition of Quaternary, orogen-parallel, extensional (or transtensional) structures with significant displacement in the Himalaya may help resolve a major question in South Asian tectonics: how do we reconcile the dramatically different Quaternary strain fields of the Himalaya and Tibet? While the Quaternary kinematics of the Himalayan orogenic wedge are dominated by southward thrusting on imbricate N-dipping thrust faults (Avouac 2003), active transcurrent and normal fault systems of the southern Tibetan Plateau primarily accommodate E-W extension (Armijo et al. 1986; Blisniuk et al. 2001). The southernmost rift systems of the plateau extend approximately as far south as the Himalayan Range crest. In the Kali Gandaki Valley, for example, the Thakkhola Graben can be traced no farther south than the area between the Annapurna and Dhaulagiri Massifs. Hurtado et al. (2001) showed that the principal growth structure of the graben (the Dangardzong Fault) lies entirely within the hanging wall of the Annapurna-Dhumpu Detachment. We suggest that Quaternary, N-dipping faults like the Annapurna-Dhumpu and Dhaulagiri Detachments serve to accommodate the strain discontinuity between southern Tibet and the Himalayan orogenic wedge, at least in central Nepal. Farther to the west, the strain discontinuity may be accommodated by predominately dextral transcurrent structures of the Karakoram and Western Nepal Fault Systems. Additional neotectonic research is needed to better understand whether similar accommodation structures also occur in the eastern Himalaya.

ACKNOWLEDGMENTS

We would like to thank B. Adams for assistance in the field and B. Chand and B. Sitaula of Earth's Paradise Treks, Travels & Geologistics for logistical support. D. K. Furlong, J. Spencer, and D. Whipp provided valuable reviews of the manuscript. This work was supported by a U.S. National Science Foundation award (EAR0711140) to K. V. Hodges and K. X Whipple.

REFERENCES CITED

Ader, T.; Avouac, J. P.; Liu-Zeng, J.; Lyon-Caen, H.; Bollinger, L.; Galetzka, J.; Genrich, J.; et al. 2012. Convergence rate across the Nepal Himalaya and interseismic coupling on the Main Himalayan Thrust: implications for seismic hazard. J. Geophys. Res. 117: B04403. doi:10.1029/2011jb009071.

Arita, K., and Ganzawa, Y. 1997. Thrust tectonics and uplift process of the Nepal Himalaya revealed from fission-track ages. J. Geogr. 106:156–167 (in Japanese).

Armijo, R.; Tapponnier, P.; Mercier, J. L.; and Han, T. L. 1986. Quaternary extension in southern Tibet: field observations and tectonic implications. J. Geophys. Res. 91:13,803–13,872.

Avouac, J. P. 2003. Mountain building, erosion, and the seismic cycle in the Nepal Himalaya. *In* Dmowska, R., ed. Advances in Geophysics. Vol. 46. San Diego, CA, Academic Press, p. 1–80.

Bernet, M. 2009. A field-based estimate of the zircon fission-track closure temperature, Chem. Geol. 259:181–189.

Blisniuk, P. M.; Hacker, B. R.; Glodny, J.; Ratschbacher, L.; Bi, S.; Wu, Z.; McWilliams, M. O.; and Calvert, A. 2001. Normal faulting in central Tibet since at least 13.5 My ago. Nature 412:628–631.

Blythe, A. E.; Burbank, D. W.; Carter, A.; Schmidt, K.; and Putkonen, J. 2007. Plio-Quaternary exhumation history of the central Nepalese Himalaya: 1. Apatite

and zircon fission track and apatite [U-Th]/He analyses. Tectonics. 26:TC3002. doi:10.1029/2006TC001990.
Bookhagen, B., and Burbank, D. W. 2010. Toward a complete Himalayan hydrological budget: spatiotemporal distribution of snowmelt and rainfall and their impact on river discharge. J. Geophys. Res. 115:F03019. doi:10.1029/2009JF001426.
Bordet, P.; Colchen, M.; Krummenacher, D.; LeFort, P.; Mouterde, R.; and Remy, M. 1971. Recherches géologiques dans l'Himalaya du Népal, région de la Thakkhola. Paris, Centre National de la Recherche Scientifique.
Braun, J. 2002. Estimating exhumation rate and relief evolution by spectral analysis of age-elevation datasets. Terra Nova 14:210–214.
———. 2005. Quantitative constraints on the rate of landform evolution derived from low-temperature thermochronology. Rev. Mineral. Geochem. 58:351–374.
Brewer, I. D.; Burbank, D. W.; and Hodges, K. V. 2003. Modeling detrital cooling-age populations: insights from two Himalayan catchments. Basin Res. 15:305–320.
———. 2006. Downstream development of detrital cooling-age signal: insights from $^{40}Ar/^{39}Ar$ muscovite thermochronology in the Nepalese Himalaya. *In* Willett, S. D.; Hovius, N.; Brandon, M. T.; and Fisher, D., eds., Tectonics, climate, and landscape evolution. Geol. Soc. Am. Spec. Pap. 398:321–338.
Brown, R. L., and Nazarchuk, J. H. 1993. Annapurna detachment fault in the Greater Himalaya of central Nepal. *In* Treloar, P. J., and Searle, M. P., eds. Himalayan tectonics. Geol. Soc. Lond. Spec. Publ. 74:461–473.
Burbank, D. W.; Blythe, A. E.; Putkonen, J.; Pratt-Situala, B.; Gabet, E.; Oskin, M.; Barros, A.; and Ojha, T. P. 2003. Decoupling of erosion and precipitation in the Himalaya. Nature 426:652–655.
Burchfiel, B. C.; Chen, Z.; Hodges, K. V.; Liu, Y.; Royden, L. H.; Deng, C.; and Xu, J. 1992. The South Tibetan detachment system, Himalayan orogen: extension contemporaneous with and parallel to shortening in a collisional mountain belt. Geol. Soc. Am. Spec. Pap. 269, 41 p.
Cattin, R., and Avouac, J. P. 2000. Modeling mountain building and the seismic cycle in the Himalaya of Nepal. J. Geophys. Res. 105:13,389–13,407.
Colchen, M.; Le Fort, P.; and Pêcher, A. 1980. Carte géologique Annapurna-Manaslu-Ganesh du Népal. Paris, Centre National de la Recherche Scientifique. Scale 1:200,000.
———. 1981. Geological map of the Annapurna-Manaslu-Ganash Himalaya of Nepal. *In* Gupta, H. K., and Delany, F. M., eds. Zagros, Hindu Kush, Himalaya: geodynamic evolution. Am. Geophys. Union Geodynamics Ser. 3. Scale 1:200,000.
———. 1986. Annapurna-Manaslu-Ganesh Himal. Paris, Centre National de la Recherche Scientifique, 136 p.
Coleman, M. E. 1996. Orogen-parallel and orogen-perpendicular extension in the central Nepalese Himalayas. Geol. Soc. Am. Bull. 108:1594–1607.
Coleman, M. E., and Hodges, K. V. 1995. Evidence for Tibetan Plateau uplift before 14 Myr ago from a new minimum age for east-west extension. Nature 374:49–52.
———. 1998. Contrasting Oligocene and Miocene thermal histories from the hanging wall and footwall of the South Tibetan detachment in the central Himalaya from $^{40}Ar/^{39}Ar$ thermochronology, Marsyandi Valley, central Nepal. Tectonics 17:726–740.
Crouzet, C.; Dunkl, I.; Paudel, L.; Arkai, P.; Rainer, T. M.; Balogh, K.; and Appel, E. 2007. Temperature and age constraints on the metamorphism of the Tethyan Himalaya in central Nepal: a multidisciplinary approach. J. Asian Earth Sci. 30:113–130.
Derry, L. A.; Evans, M. J.; Darling, R.; and France-Lanord, C. 2009. Hydrothermal heat flow near the Main Central Thrust, central Nepal Himalaya. Earth Planet. Sci. Lett. 286:101–109.
Dodson, M. H. 1973. Closure temperature in cooling geochronological and petrological systems. Contrib. Mineral. Petrol. 40:259–274.
Farley, K. A. 2000. Helium diffusion from apatite: general behavior as illustrated by Durango fluorapatite. J. Geophys. Res. 105:2903–2914.
Fort, M. 2000. Glaciers and mass wasting processes: their influence on the shaping of the Kali Gandaki Valley (higher Himalaya of Nepal). Quat. Int. 65–66:101–119.
Gaetani, M., and Garzanti, E. 1991. Multicyclic history of the northern India continental margin (northwestern Himalaya). Am. Assoc. Pet. Geol. Bull. 75:1427–1446.
Garzione, C. N.; DeCelles, P. G.; Hodkinson, D. G.; Ojha, T.; and B. N. Upreti. 2003. East-west extension and Miocene environmental change in the southern Tibetan Plateau: Thakkhola graben, central Nepal. Geol. Soc. Am. Bull. 115:3–20.
Gautheron, C.; Tassan-Got, L.; Ketcham, R. A.; and Dobson, K. J. 2012. Accounting for long alpha-particle stopping distances in (U-Th-Sm)/He geochronology: 3D modeling of diffusion, zoning, implantation, and abrasion. Geochim. Cosmochim. Acta 96:44–56.
Gehrels, G.; Kapp, P.; DeCelles, P.; Pullen, A.; Blakey, R.; Weislogel, A.; Ding, L.; et al. 2011. Detrital zircon geochronology of pre-Tertiary strata in the Tibetan-Himalayan orogen. Tectonics 30:TC5016. doi:10.1029/2011tc002868.
Gibbard, P. L.; Head, M. J.; and Walker, M. J. C. 2010. Formal ratification of the Quaternary System/Period and the Pleistocene Series/Epoch with a base at 2.58 Ma. J. Quat. Sci. 25:96–102.
Godin, L. 2003. Structural evolution of the Tethyan sedimentary sequence, central Nepal Himalaya. J. Asian Earth Sci. 22:307–328.
Godin, L.; Brown, R. L.; and Hanmer, S. 1999. High strain zone in the hanging wall of the Annapurna detachment, central Nepal Himalaya. *In* Macfarlane, A.; Sorkhabi, R. B.; and Quade, J., eds., Himalaya and Tibet: mountain roots to mountain tops. Geol. Soc. Am. Spec. Pap. 328:199–210.
Godin, L.; Gleeson, T. P.; Searle, M. P.; Ullrich, T. D.; and Parrish, R. R. 2006. Locking of southward extrusion in favour of rapid crustal-scale buckling of the Greater Himalayan sequence, Nar Valley, central Nepal. *In* Law, R. D.; Searle, M. P.; and Godin, L., eds. Channel flow: ductile extrusion and exhumation in continental collision zones. Geol. Soc. Lond. Spec. Publ. 268:269–292.

Godin, L.; Parrish, R. R.; Brown, R. L.; and Hodges, K. V. 2001. Crustal thickening leading to exhumation of the Himalayan metamorphic core of central Nepal: insight from U-Pb geochronology and $^{40}Ar/^{39}Ar$ thermochronology. Tectonics 20: 729–747.

Guillot, S.; Le Fort, P.; Pêcher, A.; Barman, M. R.; and Aprahamian, J. 1995. Contact metamorphism and depth of emplacement of the Manaslu granite (central Nepal): implications for Himalayan orogenesis. Tectonophysics 241:99–119.

Guillot, S.; Pêcher, A.; Rochette, P.; and Le Fort, P. 1993. The emplacement of the Manaslu granite of central Nepal: field and magnetic susceptibility constraints. *In* Treloar, P. J., and Searle, M. P., eds. Himalayan tectonics. Geol. Soc. Lond. Spec. Publ. 74:413–428.

Harrison, T. M.; Celerier, J.; Aikman, A. B.; Hermann, J.; and Heizler, M. T. 2009. Diffusion of ^{40}Ar in muscovite. Geochim. Cosmochim. Acta 73:1039–1051.

Herman, F.; Copeland, P.; Avouac, J. P.; Bollinger, L.; Mahéo, G.; Le Fort, P.; Rai, S.; et al. 2010. Exhumation, crustal deformation, and thermal structure of the Nepal Himalaya derived from the inversion of thermochronological and thermobarometric data and modeling of the topography. J. Geophys. Res. 115:B06407. doi:10.1029/2008JB006126.

Hodges, K. V. 2000. Tectonics of the Himalaya and southern Tibet from two perspectives. Geol. Soc. Am. Bull. 112:324–350.

Hodges, K. V.; Burchfiel, B. C.; Royden, L. H.; Chen, Z.; and Liu, Y. 1992. The metamorphic signature of contemporaneous extension and shortening in the central Himalayan orogen; data from the Nyalam transect, southern Tibet. J. Metamorph. Geol. 11:721–737.

Hodges, K. V.; Parrish, R. R.; and Searle, M. P. 1996. Tectonic evolution of the central Annapurna Range, Nepalese Himalayas. Tectonics 15:1264–1291.

Hourigan, J. K.; Reiners, P. W.; and Brandon, M. T. 2005. U-Th zonation dependent alpha-ejection in (U-Th)/He chronometry. Geochim. Cosmochim. Acta 69:3349–3365.

Huntington, K. W.; Blythe, A. E.; and Hodges, K. V. 2006. Climate change and Late Pliocene acceleration of erosion in the Himalaya. Earth Planet. Sci. Lett. 252:107–118.

Huntington, K. W., and Hodges, K. V. 2006. A comparative study of detrital mineral and bedrock age-elevation methods for determining erosion rates. J. Geophys. Res. 111:F03011. doi:10.1029/2005JF000454.

Hurtado, J. M. 2002. Tectonic evolution of the Thakkhola graben and Dhaulagiri Himalaya, central Nepal. PhD dissertation. Massachusetts Institute of Technology, Cambridge, 462 p.

Hurtado, J. M.; Hodges, K. V.; and Whipple, K. X. 2001. Neotectonics of the Thakkhola graben and implications for recent activity on the South Tibetan Fault System in the central Nepalese Himalaya. Geol. Soc. Am. Bull. 113:222–240.

Larson, K. P., and Godin, L. 2009. Kinematics of the Greater Himalayan sequence, Dhaulagiri Himal: implications for the structural framework of central Nepal. J. Geol. Soc. Lond. 166:25–43.

Le Fort, P. 1975. Himalayas: the collided range. Present knowledge of the continental arc. Am. J. Sci. 275A:1–44.

McDermott, J. A.; Whipple, K. X; Hodges, K. V.; and van Soest, M. C. 2013. Evidence for Plio-Pleistocene north-south extension at the southern margin of the Tibetan Plateau, Nyalam region. Tectonics 32:317–333. doi:10.1002/tect.20018.

Meesters, A. G. C. A., and Dunai, T. J. 2002. Solving the production-diffusion equation for finite diffusion domains of various shapes: part 1. Implications for low-temperature (U-Th)/He thermochronology. Chem. Geol. 186:333–344.

Moore, M. A., and England, P. C. 2001. On the inference of denudation rates from cooling ages of minerals. Earth Planet. Sci. Lett. 185:265–284.

Murphy, M. A.; Taylor, M. H.; Gosse, J.; Silver, C. R. P.; Whipp, D. M.; and Beaumont, C. 2014. Limit of strain partitioning in the Himalaya marked by large earthquakes in western Nepal. Nat. Geosci. 7:38–42.

Nadin, E. S., and Martin, A. J. 2012. Apatite thermochronometry within a knickzone near the Higher Himalaya front, central Nepal: no resolvable fault motion in the past one million years. Tectonics. 31: TC2010. doi:10.1029/2011TC003000.

Nakata, T. 1989. Active faults of the Himalaya of India and Nepal. *In* Malinconico, L. L., and Lillie, R. J., eds. Tectonics of the western Himalayas. Geol. Soc. Am. Spec. Pap. 232:243–264.

Nazarchuk, J. H. 1993. Structure and geochronology of Greater Himalaya, Kali Gandaki region, west-central Nepal. MS thesis, Carleton University, Ottawa, Canada, 157 p.

Pandey, M. R., Tandukar, R. P.; Avouac, J. P.; Lavé, J.; and Massot, J. P. 1995. Interseismic strain accumulation on the Himalayan crustal ramp (Nepal). Geophys. Res. Lett. 22:751–754.

Pêcher, A. 1978. Déformation et métamorphisme associés à une zone de cisaillement: example du grand chevauchement central Himalayen (MCT). DSc thesis, Université de Grenoble.

Reiners, P. W., and Brandon M. T. 2006. Using thermochronology to understand orogenic erosion. Annu. Rev. Earth Planet. Sci. 34:419–466. doi:10.1146/annurev.earth.34.031405.125202.

Reiners, P. W.; Spell, T. L.; Nicolescu, S.; and Zanetti, K. A. 2004. Zircon (U-Th)/He thermochronometry: He diffusion and comparisons with $^{40}Ar/^{39}Ar$ dating. Geochim. Cosmochim. Acta 68:1857–1887.

Robert, X.; van der Beek, P.; Braun, J.; Perry, C.; Dubille, M.; and Mugnier, J.-L. 2009. Assessing Quaternary reactivation of the Main Central thrust zone (central Nepal Himalaya): new thermochronologic data and numerical modeling. Geology 37:731–734.

Ruhl, K. W., and Hodges, K. V. 2005. The use of detrital mineral cooling ages to evaluate steady-state assumptions in active orogens: an example from the central

Nepalese Himalaya. Tectonics. 24:TC4015. doi:10.1029/2004TC001712.

Searle, M. P., and Godin, L. 2003. The South Tibetan Detachment and the Manaslu leucogranite: a structural reinterpretation and restoration of the Annapurna-Manaslu Himalaya, Nepal. J. Geol. 111:505–523.

Searle, M. P.; Noble, S. R.; Hurford, A. J.; and Rex, D. C. 1999. Age of crustal melting, emplacement and exhumation history of the Shivling leucogranite, Garhwal Himalaya. Geol. Mag. 136:513–525.

Searle, M. P.; Simpson, R. L.; Law, R. D.; Parrish, R. R.; and Waters, D. J. 2003. The structural geometry, metamorphic, and magmatic evolution of the Everest massif, High Himalaya of Nepal–South Tibet. J. Geol. Soc. Lond. 160:345–366.

Shuster, D. L.; Flowers, R. M.; and Farley, K. A. 2006. The influence of natural radiation damage on helium diffusion kinetics in apatite. Earth Planet. Sci. Lett. 249:148–161.

Silver, C. R. P. 2012. The Dhaulagiri Transtentional Zone: an active fault zone within the western Nepalese Himalaya. MS thesis, University of Houston, 66 p.

Spiegel, C.; Kohn, B.; Belton, D.; Berner, Z.; and Gleadow, A. 2009. Apatite (U-Th-Sm)/He thermochronology of rapidly cooled samples: the effect of He implantation. Earth Planet. Sci. Lett. 285:105–114.

Streule, M. J.; Carter, A.; Searle, M. P.; and Cottle, J. M. 2012. Constraints on brittle field exhumation of the Everest-Makalu section of the Greater Himalayan sequence: implications for models of crustal flow. Tectonics. 31:TC3010. doi:10.1029/2011TC003062.

Styron, R. H.; Taylor, M. H.; and Murphy, M. A. 2011. Oblique convergence, arc-parallel extension, and the role of strike-slip faulting in the High Himalaya. Geosphere 7:582–596.

Thiede, R. C., and Ehlers, T. A. 2013. Large spatial and temporal variations in Himalayan denudation. Earth Planet. Sci. Lett. 371–372:278–293.

Vannay, J. C., and Hodges, K. V. 1996. Tectonometamorphic evolution of the Himalayan metamorphic core between the Annapurna and Dhaulagiri, central Nepal. J. Metamorph. Geol. 14:635–656.

Whipp, D. M., and Ehlers, T. A. 2007. Influence of groundwater flow on thermochronometer-derived exhumation rates in the central Nepalese Himalaya. Geology 35:851–854.

Whipp, D. M.; Ehlers, T. A.; Blythe, A. E.; Huntington, K. W.; Hodges, K. V.; and Burbank, D. W. 2007. Plio-Quaternary exhumation history of the central Nepalese Himalaya: 2. Thermo-kinematic and thermochronometer age prediction model. Tectonics. 26:TC3003. doi:10.1029/2006TC001991.

Whipp, D. M.; Ehlers, T. A.; Braun, J.; and Spath, C. D. 2009. Effects of exhumation kinematics and topographic evolution on detrital thermochronometer data. J. Geophys. Res. 114:F04021. doi:10.1029/2008JF001195.

Willett, S. D., and Brandon, M. T. 2013. Some analytical methods for converting thermochronometric age to erosion rate. Geochem. Geophys. Geosyst. 14:209–222. doi:10.1029/2012GC004279.

Wobus, C.; Heimsath, A.; Whipple, K.; and Hodges, K. 2005. Active out-of-sequence thrust faulting in the central Nepalese Himalaya. Nature 434:1008–1010.

Wu, C.; Nelson, K.; Wortman, G.; Samson, S.; Yue, Y.; Li, J.; Kidd, W.; and Edwards, M. 1998. Yadong cross structure and South Tibetan Detachment in the east central Himalaya (89°–90°E). Tectonics 17:28–45.